Reaction front for $A + B \rightarrow C$ diffusion-reaction systems with initially separated reactants

Hernan Larralde and Mariela Araujo
Center for Polymer Studies and Department of Physics, Boston University, Boston, Massachusetts 02215

Shlomo Havlin
Department of Physics, Bar-Ilan University, Ramat-Gan, Israel and Center for Polymer Studies and Department of Physics, Boston University, Boston, Massachusetts 02215

H. Eugene Stanley
Center for Polymer Studies and Department of Physics, Boston University, Boston, Massachusetts 02215
(Received 14 February 1992)

We study both analytically and numerically the $A + B \rightarrow C$ diffusion-reaction system for the case of initially separated reactants. We find the functional forms of the reaction front and also of the concentration profiles of the reactants. The profile of the production rate $R(x,t)$ at site x and time t scales as $t^{-2/3}(x/t^{1/6})^{3/4}\exp[-\frac{2}{3}(\lambda x/t^{1/6})^{3/2}]$ for the spatial range $t^{1/6} \ll x \ll t^{1/2}$. Our results are supported by numerical solutions of the diffusion-reaction equation, and are in agreement with Monte Carlo simulations in dimension $d = 2$.

PACS number(s): 05.40.+j, 05.60.+w, 66.10.Cb, 82.20.Wt

There has been much recent interest in the characteristics and the kinetics of diffusion-reaction systems of the type $A + B \rightarrow C$, where the reactants are allowed to diffuse, and the products C are inert immobile particles [1–7]. In particular, several theoretical and experimental studies have focused on the situation in which the reactants are initially separated in space [8–14]. These systems develop a reaction front at the "interface" of the reactants, which is marked by the C particles. This reaction front should be relevant for a variety of biological, chemical, and physical systems [15–22].

In this paper we derive the functional form of the reaction front; we compare this form with exact numerical analysis, as well as with Monte Carlo (MC) simulations of the diffusion-reaction systems. We find good agreement between the the MC simulations in $d = 2$ and the theoretical results.

The equations that are used to describe diffusion-reaction systems are [2, 8, 10–12, 14]

$$\frac{\partial C_A}{\partial t} = D_A \frac{\partial^2 C_A}{\partial x^2} - kC_A C_B, \tag{1}$$

$$\frac{\partial C_B}{\partial t} = D_B \frac{\partial^2 C_B}{\partial x^2} - kC_A C_B, \tag{2}$$

where $C_A \equiv C_A(x,t)$ and $C_B \equiv C_B(x,t)$ are the concentrations of A and B particles at position x and time t, respectively, and k is the reaction constant. The rate of production $R(x,t)$ of C particles is given by

$$R \equiv kC_A C_B. \tag{3}$$

It is widely believed that Eqs. (1), (2), and (3) represent realistic diffusion-reaction systems in $d \geq 2$ and they have led to certain scaling hypotheses for the reaction front $R(x,t)$ which appear to be valid for systems of dimension $d = 2, 3$ (but not for $d = 1$) [8–14].

We will consider the case in which both diffusion constants are equal, and initially the A particles are uniformly distributed to the right of the origin while the B particles are uniformly distributed to the left of the origin with equal concentrations c_0. If we define $F(x,t) \equiv C_A(x,t) - C_B(x,t)$, then

$$\frac{\partial F}{\partial t} = D\frac{\partial^2 F}{\partial x^2}, \tag{4}$$

which—given the initial conditions—has the solution

$$F(x,t) = c_0 \operatorname{erf}\left(\frac{x}{\sqrt{4Dt}}\right). \tag{5}$$

Next we rewrite the concentrations of A and B particles as follows (see Fig. 1):

$$C_A(x,t) = G_1(x,t) + \delta C(x,t), \tag{6}$$

$$C_B(x,t) = G_2(x,t) + \delta C(x,t), \tag{7}$$

where

$$G_1(x,t) = \begin{cases} c_0 \operatorname{erf}(x/\sqrt{4Dt}) & [x > 0] \\ 0 & [x < 0] \end{cases} \tag{8}$$

and

$$G_2(x,t) = -G_1(-x,t). \tag{9}$$

Substituting $C_A(x,t)$ and $C_B(x,t)$ in Eq. (1) yields

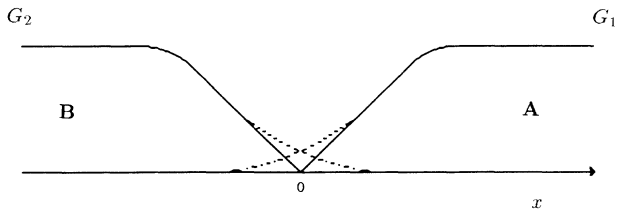

FIG. 1. Schematic picture of the reactant concentration profiles near the origin. The solid lines represent the $G_{1,2}(x,t)$ part of the profile; the dashed lines represent the complete form $G_{1,2}(x,t)+\delta C(x,t)$. Note that the profile of species A is given solely by $\delta C(x,t)$ on the left of the origin.

$$\frac{\partial(\delta C)}{\partial t}=D\frac{\partial^2(\delta C)}{\partial x^2}-k\left[c_0\ \mathrm{erf}\left(\frac{x}{\sqrt{4Dt}}\right)+\delta C\right]\delta C. \tag{10}$$

Thus we have reduced the coupled Eqs. (1), (2), and (3) to a single equation, Eq. (10). Note that $\delta C(x,t)$ is an even function of x, yet if we assume that the concentration profiles $C_A(x,t)$ and $C_B(x,t)$ are smooth, then $\delta C(x,t)$ is not differentiable at the origin. Equation (10) is still an intractable nonlinear differential equation, but if we focus on the region $x \ll \sqrt{4Dt}$, and assume that we are still far enough from the origin so that δC is negligible compared to $(c_0/\sqrt{\pi Dt})x$ (Fig. 1), then Eq. (10) reduces to

$$\frac{\partial(\delta C)}{\partial t}=D\frac{\partial^2(\delta C)}{\partial x^2}-k\left(c_0\frac{x}{\sqrt{\pi Dt}}\right)\delta C. \tag{11}$$

Let us consider the equation

$$D\frac{\partial^2(\delta C)}{\partial x^2}-ka\frac{x}{t^{1/2}}(\delta C)=0, \tag{12}$$

where $a \equiv c_0/(\pi D)^{1/2}$. The solution to this equation that vanishes as $x \to \infty$ is

$$\delta C(x,t)=f(t)\ \mathrm{Ai}\left(\lambda\frac{x}{t^{1/6}}\right), \tag{13}$$

where $\lambda=(ka/D)^{1/3}$, $\mathrm{Ai}(z)$ is an Airy function, and $f(t)$ is a function only of time. To determine $f(t)$, we equate the right-hand side (RHS) of Eq. (10) with 0, take the linear approximation for the error function as before, and demand that δC can be written as $\delta C(x,t)=t^{\alpha}B(x/t^{1/6})$. This immediately gives $\alpha=-\frac{1}{3}$. Thus, the solution for (12) will be given by

$$\begin{aligned}\delta C(x,t) &\sim t^{-1/3}\mathrm{Ai}\left(\lambda\frac{x}{t^{1/6}}\right)\\ &\sim t^{-1/3}\left(\frac{x}{t^{1/6}}\right)^{-1/4}\exp\left[-\frac{2}{3}\left(\frac{\lambda x}{t^{1/6}}\right)^{3/2}\right].\end{aligned} \tag{14}$$

As may be confirmed by direct substitution, this expression is a solution of Eq. (11) up to terms of order $(\delta C)/t$ (which can be neglected for large t). Also, given the nature of the Airy function, we can be sure that δC is negligible with respect to $ax/\sqrt{t}$ for $\lambda x \gg t^{1/6}$ supporting the argument leading to (11). Thus we expect Eq. (14) to be the solution of (10) at long times within the region $t^{1/6}/\lambda \ll x \ll t^{1/2}/a$.

Using Eq. (14) we can write an expression for the reaction front $R(x,t)$ defined in (3). Since we are in the region $\lambda x \gg t^{1/6}$ we use the asymptotic expression for Ai(z) and find

$$\begin{aligned}R(x,t) &\simeq \frac{kax}{t^{1/2}}(\delta C)\\ &\sim t^{-2/3}\left(\frac{x}{t^{1/6}}\right)^{3/4}\exp\left[-\frac{2}{3}\left(\frac{\lambda x}{t^{1/6}}\right)^{3/2}\right].\end{aligned} \tag{15}$$

Equation (15) is consistent with the exponents derived in Ref. [8] using scaling arguments. The width of the reaction front grows as $t^{1/6}$, whereas the height can be identified with the prefactor $t^{-2/3}$ in Eq. (15). However, (15) provides a more quantitative solution of Eqs. (1), (2), and (3) than the previous scaling arguments [8], as well as information on the dependence of the form of the reaction front on the parameters c_0, k, and D.

The concentration of product particles C can immediately be calculated as the integral over time of the reaction front R,

$$\begin{aligned}I(x,t) &\equiv \int^t R(x,t')dt'\\ &\sim t^{1/3}\left(\frac{x}{t^{1/6}}\right)^{-3/4}\exp\left[-\frac{2}{3}\left(\frac{\lambda x}{t^{1/6}}\right)^{3/2}\right].\end{aligned} \tag{16}$$

The region $x \gg \sqrt{4Dt}$ is also amenable to analysis. In this region, δC is extremely small and the error function is well approximated by 1; thus Eq. (10) becomes

$$\frac{\partial(\delta C)}{\partial t}=D\frac{\partial^2(\delta C)}{\partial x^2}-kc_0(\delta C). \tag{17}$$

This equation is precisely what one would expect in the extremely rare cases that a particle manages to diffuse very far into the domain of the other particles. Yet this region is of little interest since in general R is extraordinarily small.

Equations (14)–(16) can now be directly compared with exact numerical analysis of Eqs. (1)–(3), as well as with measurements of the reaction front from MC simulations of the diffusion-reaction system. We check the validity of the approximations by solving Eqs. (1)–(3) using exact enumeration of the discrete version of these equations.

Following Taitelbaum *et al.* [12], we consider a discrete lattice in one dimension, with initially one particle A per site on the left of the origin and one B per site on the right. We update the concentrations by first considering solely the diffusive step, and then take into account the possible reactions. Thus, for step n, we write

$$\Gamma_n(x)=(1-p)C_A(n,x)+\frac{p}{2}[C_A(n,x+1)+C_A(n,x-1)], \tag{18}$$

$$\Omega_n(x)=(1-p)C_B(n,x)+\frac{p}{2}[C_B(n,x+1)+C_B(n,x-1)], \tag{19}$$

where p is the probability that a particle takes a step. We then include the reaction by writing the concentrations at position x and step $n+1$ as

$$C_A(n+1,x) = \Gamma_n(x)[1-\theta_A(n,x)], \tag{20}$$

$$C_B(n+1,x) = \Omega_n(x)[1-\theta_B(n,x)], \tag{21}$$

where θ_A and θ_B are defined by

$$\theta_i \equiv \begin{cases} \min\left[\frac{C_j\,[1-Q(1)]}{C_A-C_BQ(1)},1\right], & [C_A \neq C_B] \\ \frac{C_A\,k}{1+C_Ak}, & [C_A = C_B]. \end{cases} \tag{22}$$

Here i denotes species A and j denotes species B and vice versa; $Q(\tau)$ is given by

$$Q(\tau) \equiv \exp[-k(C_A - C_B)\tau]. \tag{23}$$

Here we take τ as the unit time step [12]. We note that in the continuum limit Eqs. (20) and (21) reduce to Eqs. (1) and (2). The reaction front R will be given by

$$R = \frac{C_AC_B[1-Q(1)]}{C_A - C_BQ(1)}. \tag{24}$$

In Figs. 2–4 we plot C_A, R, and I calculated from Eqs. (20), (21), and (24) in the scaling form suggested by Eqs. (14), (15), and (16). The large linear region in these plots confirms our predictions within the range $t^{1/6} \ll x \ll t^{1/2}$. In the region $x \gg t^{1/2}$, the form of R calculated from Eq. (24) appears to be an exponential in x, which

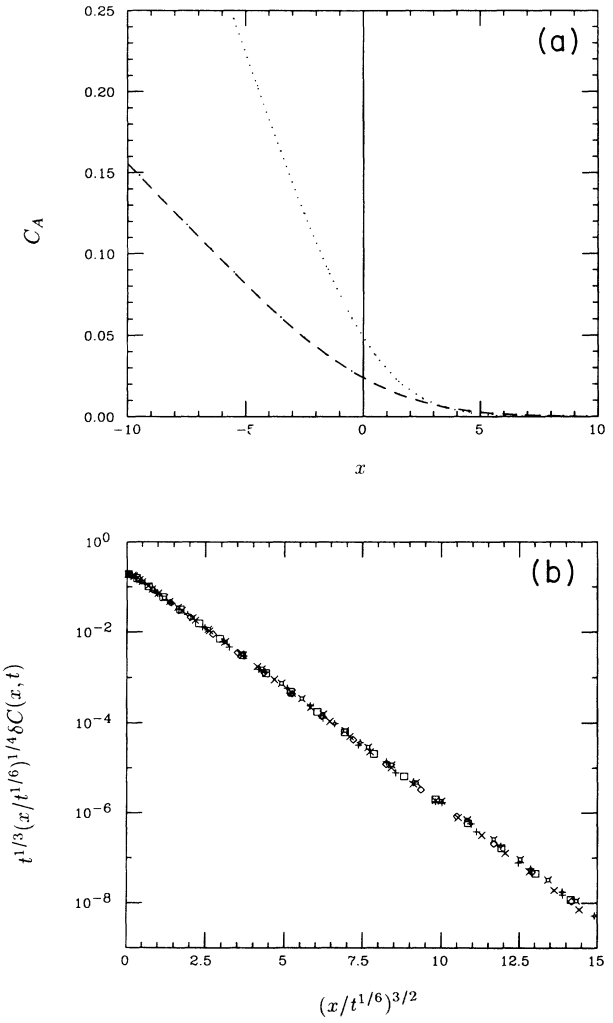

FIG. 2. (a) Concentration profile $C_A(x,t)$ near the origin for times 0 (solid line), 500 (dotted line), and 4000 (dashed line) obtained by exact enumeration of Eqs. (20) and (21). (b) Scaling plot of the numerical solution of (1) in the form given in Eq. (14) for $C_A(x,t)$ for $x \geq 0$ and a sequence of times, $t =$ 250 (+), 500 ($\diamond$), 1000 ($\oplus$), 2000 (+), 4000 ($\Box$), and 8000 ($\boxtimes$). The data were obtained by exact enumeration of Eqs. (20) and (21). The large linear regime confirms our results in the region governed by Eq. (14).

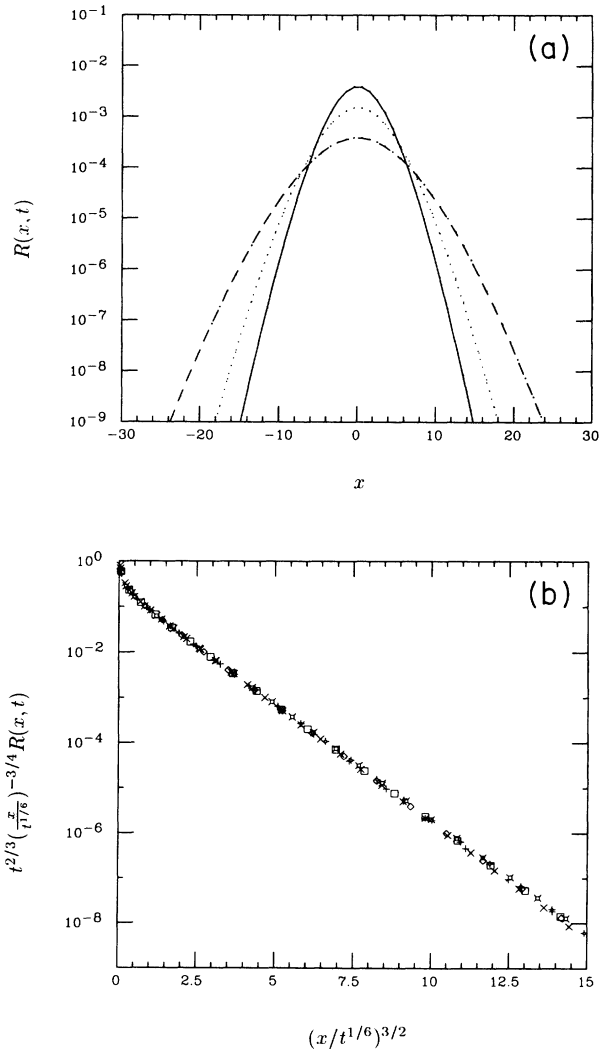

FIG. 3. (a) Reaction front profile $R(x,t)$ near the origin calculated by exact enumeration of Eqs. (20) and (21) for various times $t = 250$ (solid line), 500 (dotted line), and 1000 (dashed line). (b) Scaling plot of $R(x,t)$ obtained from exact enumeration, using the form suggested by Eq. (15). Symbols are the same as for Fig. 2(b).

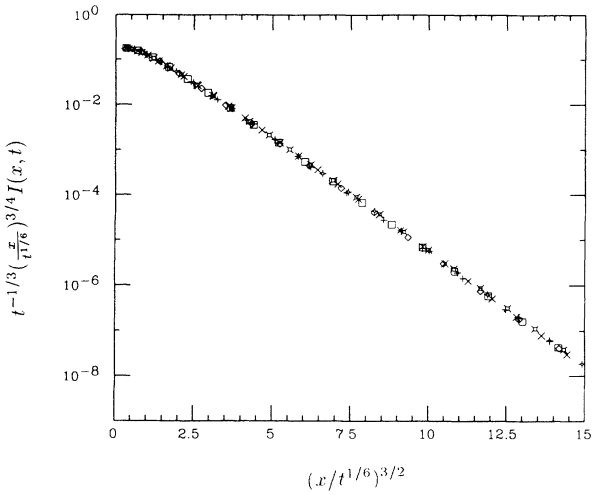

FIG. 4. Scaling plot of $I(x,t)$ calculated from Eqs. (20) and (21). The large linear regime agrees with the prediction of Eq. (16). Symbols are the same as for Fig. 2(b).

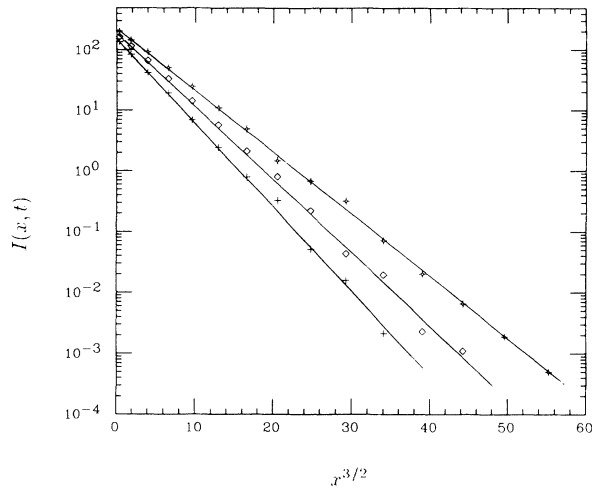

FIG. 6. $I(x,t)$ calculated by MC simulations in $d = 2$, with reaction probability equal to 1 (this corresponds to taking the limit $k \to \infty$). The linear regime in this plot suggests that Eq. (16) properly describes the shape of $I(x,t)$, but with an effective (finite) reaction constant k. Here calculations for three different times are shown, $t = 250$ (+), 500($\diamond$), and 1000 ($\oplus$).

is consistent with Eq. (17) (Fig. 5).

We also performed MC simulations of the same system in two dimensions, under the condition of certain reaction, i.e., every time A and B meet, they react with probability 1. This corresponds to the limit $k \to \infty$ in Eqs. (1)–(3) and Eqs. (20) and (21). According to our results, this condition should lead to an extremely narrow (in principle a δ function) reaction front, which is certainly not the case in the simulations. However, if we identified these systems with an effective finite reaction constant k, the shape of the integrated reaction front appears to be consistent with Eq. (16) (Fig. 6).

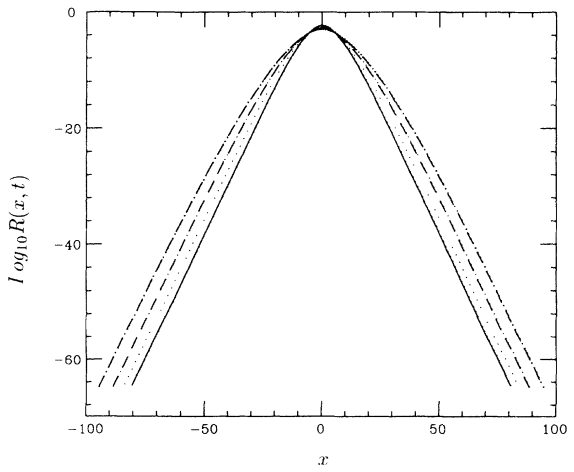

FIG. 5. Plot analogous to Fig. 3(a), except that the scale is extended to regions where $x \gg \sqrt{4Dt}$ and $R(x,t)$ is very small; here $t = 250$ (solid line), 500 (dotted line), 1000 (dashed line), and 2000 (dot-dashed line). Note that the profiles tend to exponentials, which is consistent with Eq. (17).

To conclude, we have derived the functional form of the reaction front for diffusion-reaction systems with initially separated reactants, from the equations believed to describe these systems at least in two and three dimensions. We confirmed our results numerically, but found that actual MC simulations of these systems apparently are properly described by these equations assuming an effective finite value for the reaction constant k. This effective k must somehow reflect the presence of concentration fluctuations that arise from the microscopic diffusive process (presumably each particle performs a random walk). It is also important to note that for one-dimensional systems not only do the scaling exponents not agree [11, 13] with those derived from Eqs. (1)–(3), but also the form of the reaction front appears to be better fitted by the form [13]

$$I(x,t) \sim t^{1-\beta} \exp\left[-\nu\left(\frac{|x|}{t^{\alpha}}\right)\right], \quad [d=1], \tag{25}$$

where $\alpha \simeq 0.3$ and $\beta \simeq 0.8$ [13]. Our results leave open the question of which is the correct theoretical description of these systems, which should take into account the correlations and the fluctuations in the concentrations, both of which seem to play a crucial role in $d = 1$, and in the value of the reaction constant for all dimensions.

We thank G. Huber for a critical reading of the manuscript. The Center for Polymer Studies is supported by grants from NSF and ONR. H.L. acknowledges support of CONACYT Mexico, M.A. the support of Intevep S.A, while S.H. thanks the U.S.–Israel Binational Science Foundation for partial support.

[1] M. v. Smoluchowski, Z. Phys. Chem. **29**, 129 (1917).
[2] S. A. Rice, *Diffusion-Controlled Reactions* (Elsevier, Amsterdam, 1985).
[3] A. A. Ovchinnikov and Ya. B. Zel'dovich, Chem Phys. **28**, 215 (1978).
[4] D. Toussaint and F. Wilczek, J. Chem. Phys. **78**, 2642 (1983).
[5] P. Meakin and H. E. Stanley, J. Phys. A **17**, L173 (1984); K. Kang and S. Redner, Phys. Rev. Lett. **52**, 955 (1984).
[6] M. Bramson and J. Lebowitz, Phys. Rev. Lett. **61**, 2397 (1988); I. Sokolov, H. Schnorer, and A. Blumen, Phys. Rev. A **44**, 2388 (1991).
[7] R. Kopelman, J. Stat. Phys. **42**, 201 (1986).
[8] L. Galfi and Z. Racz, Phys. Rev. A **38**, 3151 (1988).
[9] Y. E. Koo, L. Li, and R. Kopelman, Mol. Cryst. Liq. Cryst. **183**, 187 (1990); Y. E. Koo and R. Kopelman, J. Stat. Phys. **65**, 893 (1991).
[10] Z. Jiang and C. Ebner, Phys. Rev. A **42**, 7483 (1990).
[11] S. Cornell, M. Droz, and B. Chopard, Phys. Rev. A **44**, 4826 (1991).
[12] H. Taitelbaum, S. Havlin, J. E. Kiefer, B. L. Trus, and G. H. Weiss, J. Stat. Phys. **65**, 873 (1991).
[13] M. Araujo, S. Havlin, H. Larralde, and H. E. Stanley, Phys. Rev. Lett. **68**, 1791 (1992).
[14] E. Ben-Naim and S. Redner (unpublished).
[15] D. Avnir and M. Kagan, Nature **307**, 717 (1984), and references cited therein.
[16] G. T. Dee, Phys. Rev. Lett. **57**, 275 (1986).
[17] B. Heidel, C. M. Knobler, R. Hilfer, and R. Bruinsma, Phys. Rev. Lett. **60**, 2492 (1986).
[18] R. E. Liesegang, Naturwiss. Wochensch. **11**, 353 (1896).
[19] T. A. Witten and L. M. Sander, Phys. Rev. Lett. **47**, 1400 (1981).
[20] K. F. Mueller, Science **225**, 1021 (1984).
[21] R. A. Ball, Aust. Gemmol. **12**, 89 (1974).
[22] See, e.g., the chapters by B. Sapoval and by J.-F. Gouyet *et al.* in *Fractals and Disordered Systems*, edited by A. Bunde and S. Havlin (Springer-Verlag, Berlin, 1991).